

# Investigation of density of states and charge carrier mobility in amorphous semiconductors via time-of-flight photocurrent analysis

F. Serdouk , A. Boumali †, M. L. Benkhedir ‡, Y. Goutal §

Laboratory of Theoretical and Applied Physics, Echahid Cheikh Larbi Tebessa University, Tebessa, Algeria

Received February 11, 2025, in final form September 25, 2025

The present study examines the electronic transport characteristics of amorphous semiconductors through ToF measurements and numerical simulations. The primary objective is to determine the DOS in amorphous selenium (a-Se) and to assess the temperature and electric field dependence of the hole mobility. A comprehensive investigation of localized states within the mobility gap is performed using Laplace transform analysis of ToF photocurrent transients, combined with the multiple trapping model. This approach enables accurate reconstruction of the DOS across a wide temperature range, allowing clear identification of shallow and deep trap levels and revealing thermally activated transport mechanisms. Simulated ToF currents are also used to evaluate the hole drift mobility under various thermal and field conditions. Activation energies are extracted from Arrhenius plots of the mobility data. The results support a physically consistent description of the electronic structure in a-Se and validate the applicability of Laplace-based techniques for probing charge transport in disordered semiconductors.

**Key words:** *amorphous selenium (a-Se), time-of-flight (TOF), transient photocurrent (TPC), Laplace transform analysis, multiple trapping model (MTM), density of states (DOS)*

## 1. Introduction

Amorphous semiconductors, especially amorphous selenium (a-Se), have attracted considerable interest owing to their distinctive electrical characteristics and practical uses in devices like photoreceptors and X-ray detectors. In contrast to crystalline semiconductors, a-Se exhibits an absence of long-range order, leading to a wide distribution of localized states inside its mobility gap. Comprehending the electronic transport characteristics of a-Se, including the DOS and charge carrier mobility is essential for enhancing its efficacy in electrical and optoelectronic devices. The movement of charge within a dielectric substance is crucial in numerous electrical and photographic systems. A comprehensive understanding of process dynamics can yield significant insights into the electrical structure of the material. The temporal rate of charge displacement and the efficiency of their creation by light or energetic electrons have been investigated experimentally using a ToF technique (for further details on this technique, see to [1–5]).

The assessment of the DOS in amorphous semiconductors yields significant understanding of the energy distribution of localized states, which serve as trapping foci for charge carriers. These states profoundly affect the transport parameters and are essential for comprehending charge recombination, trapping, and detrapping procedures. This study aims at characterizing the DOS in amorphous selenium (a-Se) utilizing modern methodologies, including Laplace transform analysis of transient photocurrent (TPC) data, alongside ToF (ToF) measurements to evaluate the hole mobility. The ToF approach is

\*fadila.serdouk@univ-tebessa.dz

†Corresponding author: boumali.abdelmalek@gmail.com.

‡benkhedir@gmail.com

§yazid.gouttel@univ-tebessa.dz

among the most prevalent methods for quantifying the charge carrier mobility in disordered materials such as a-Se. In a standard ToF experiment, a brief pulse of light produces electron-hole pairs within the material. An applied electric field induces a drift of charge carriers, and their transit time is measured as they traverse the material.

The mobility  $\mu$  of the charge carriers is determined using the equation  $\mu = L/F \cdot t_{tr}$ , where  $L$  represents the sample thickness,  $F$  denotes the applied electric field, and  $t_{tr}$  signifies the transit time. The ToF approach delivers direct data regarding charge transport characteristics, elucidating the aspects of carrier movement, trap distribution, and the characteristics of localized states. The ToF approach is especially advantageous for amorphous semiconductors as it differentiates between dispersive and non-dispersive transport. In dispersive transport, carriers undergo considerable trapping, resulting in a spreading of the current pulse, whereas in nondispersive transport, carriers display uniform motion with a precise transit time, commonly seen in materials with few traps or isolated states. Consequently, the duration-of-Flight ToF measuring technique is an essential instrument for assessing the transit duration of mobile entities and is extensively used to investigate the charge carrier transport characteristics in diverse condensed materials, encompassing both inorganic and organic semiconductors. The resultant transient current elucidates the transit duration and offers insights into dynamic processes during the charge transport through the sample, including carrier trapping and release in trap states, carrier diffusion, and percolation (for further details, see to [6–9]).

Schmidlin and Noolandi [2, 3] proposed the multiple-trapping model (MTM) to elucidate the dynamic behavior of charge carriers in a sample through traditional sets of linked kinetic equations governing trapping and heat release rates. This method can precisely reproduce the experimental current signal  $I(t)$  when appropriate parameters for trapping and release rates are presumed. The MTM has been extensively and effectively utilized to examine transient current decays in both inorganic and diverse organic semiconductors. These films comprise amorphous inorganic or organic semiconductors, employing suitable assumptions for trapping and release parameters represented by a continuous distribution of trap states, including exponential  $e^{-E/k_B T}$ , Gaussian, or other trap distributions. This strategy is effective only when the selected trap distribution shape appropriately represents the localized states that predominate the trapping occurrences [10–12].

Naito et al. [11–14] introduced a spectroscopic technique to derive localized-state distributions by examining transient photo-current data acquired via transient photoconductivity or the ToF method, employing the Laplace transform within a multiple-trapping model and applying appropriate approximations. The Laplace transform-based method presents multiple advantages compared to alternative techniques: (i) it effectively extracts localized-state distributions for materials exhibiting either nondispersive or dispersive transport; the analysis is both computationally efficient and rapid, and (ii) it facilitates the extraction of localized-state distributions from both the pre- and post-monomolecular recombination phases in transient photoconductivity, as well as from both pre- and post-transit time phases in ToF photo-current transients. This facilitates an expanded measurement range of localized-state distributions.

A series of comprehensive and influential studies significantly advanced the understanding of localized states in amorphous selenium (a-Se). By employing multiple experimental techniques, these works probed the electronic structure of a-Se and initiated a scientific debate regarding the symmetry — or asymmetry — of the density of localized states (DOS) near the band edges. In particular, by analyzing both the pre-transit and post-transit regimes of ToF photocurrents, Benkhedir et al. [15–19] demonstrated the effectiveness of transient current analysis in revealing the distribution of trap states on both sides of the bandgap.

Building on this foundational work, the present study focuses specifically on pure stabilized amorphous selenium and aims at refining the understanding of the density of localized states in the conduction band tail. Our methodology introduces several key advancements over the prior approaches. Firstly, we apply a Laplace transform to the entire ToF photocurrent signal, without isolating specific temporal regions (e.g., pre- or post-transit), thereby preserving the full dynamics of charge transport. Secondly, our measurements span a wide range of temperatures, allowing access to thermally activated transport regimes and providing finer energy resolution in the extracted DOS. This technique enables a direct, assumption-free reconstruction of the conduction band DOS, in contrast to earlier methods based on iterative fitting and predefined functional forms [20].

This study provides a detailed temperature-resolved extraction of the conduction band density of

localized states (DOS) in pure amorphous selenium using a Laplace transform-based analysis of ToF currents — an approach that offers enhanced resolution and physical insight compared to the previous models. By addressing the limitations of earlier methods and enriching the understanding of the electronic structure in a-Se, this work strengthens the theoretical and experimental foundations for modelling the charge transport in disordered semiconductors.

To assess the physical plausibility of the extracted DOS and to explore a potential symmetry between conduction and valence band tails, we rely on our previously developed model near the valence band edge. This framework is employed to simulate ToF transients and investigate how hole mobility evolves with temperature and electric field. The corresponding numerical estimations are presented, along with an analysis of the Poole–Frenkel effect and derived activation energies. Unlike earlier assumptions [21], which suggested a monotonously increasing DOS extending up to 0.55 eV above the valence band edge, our results point to a more localized distribution of states, offering a better alignment with the experimental transport behavior.

By comparing the conduction band DOS extracted in this work with the simulated behavior based on the valence band model, we aim at providing a unified and physically consistent description of the localized states in a-Se, and at reevaluating the assumption of symmetry between both band tails under controlled experimental conditions. In this context, the present work offers an alternative extraction approach and provides a detailed examination of existing DOS models, with the aim of supporting further progress in the understanding and modelling the charge transport in disordered semiconductors.

## 2. Review of the laplace transform method for ToF photocurrent

### 2.1. Theory

In ToF measurements, a thin film of amorphous semiconductors is positioned between two electrodes, with at least one electrode serving as a barrier to carrier injection. A brief pulse of highly absorbed light stimulates a small layer of electron-hole pairs via one of the electrodes. Depending on the polarity of the applied electric field, either holes or electrons are induced into the bulk of the material. The carriers subsequently arrive at the opposing electrode within a specific transit time,  $t_r$ , which is recognized as either a swift decrease in the transient photocurrent for nondispersive transport or an inflection point in the double logarithmic representation of the transient photocurrent for dispersive transport.

Several assumptions are established for the ToF Laplace Transform (LT) analysis: (i) The transport of photogenerated carriers transpires through a trap-controlled band transport mechanism; (ii) the mobile carriers consist of either holes or electrons; (iii) all localized states exhibit uniform capture cross sections; and (iv) the localized states remain unsaturated, a condition commonly observed during ToF transient photocurrent measurements under small-signal conditions. The essential equations for the trap-controlled band transport mechanism are articulated as [2, 3]:

$$\frac{\partial p(x, t)}{\partial t} = - \sum_i \mu \frac{\partial p_i(x, t)}{\partial t} - \mu_0 F \frac{\partial p(x, t)}{\partial x} + p_0 \delta(t) \delta(x), \quad (2.1)$$

$$\frac{\partial p_i(x, t)}{\partial t} = \omega_i p(x, t) - \gamma_i p_i(x, t). \quad (2.2)$$

In this context,  $x$  denotes the distance from the lighted surface,  $p(x, t)$  signifies the free carrier density at location  $x$  and time  $t$ , whereas  $p_i(x, t)$  represents the trapped carrier density at the  $i$ -th localized state. In this context,  $p_0$  represents the injected free carrier density per unit area, while  $\omega_i = \sigma_p v_{\text{th}} g(E_i) \cdot \Delta E$  represents the capture rate constant at the  $i$ -th localized state,  $\gamma_i = v \exp(-E_i/k_B T)$  denotes the release rate constant at the  $i$ -th localized state,  $\sigma_p$  signifies the capture cross section,  $v_{\text{th}}$  indicates the thermal velocity,  $v$  is the attempt-to-escape frequency,  $E_i = i\Delta E$  is the  $i$ -th energy level below (or above) a mobility edge,  $g(E_i)$  refers to the DOS at the  $i$ -th localized state, and  $\delta(t)$  and  $\delta(x)$  are Dirac delta functions that establish the initial conditions for the ToF experiment. These equations can be resolved via Laplace transforms. The Laplace domain solution for  $\hat{p}(x, s)$  is provided by (see to [11–14] for further

details):

$$\hat{p}(x, s) = \frac{p_0}{\mu_0 F} \exp\left(-\frac{a(s)t_0 x}{L}\right), \quad (2.3)$$

where:

$$a(s) = s \left[ 1 + \sum_i \frac{\omega_i}{s + g_i} \right] = s \left[ 1 + \int_0^{E_{\text{mid}}} \frac{\sigma_p v_{\text{th}} g(E)}{s + v \exp(-E/k_B T)} dE \right], \quad (2.4)$$

with  $t_0 = \frac{L}{\mu_0 F}$  and  $E_{\text{mid}}$  representing the midgap energy and  $L$  being the sample thickness. Differentiating  $a(s)$  with respect to  $\ln(s)$  gives:

$$\frac{da(s)}{d \ln(s)} = s \left[ 1 + \int_0^{E_{\text{mid}}} \sigma_p v_{\text{th}} g(E) h(s, E) dE \right], \quad (2.5)$$

with

$$h(s, E) = \frac{v \exp(-E/k_B T)}{[s + v \exp(-E/k_B T)]^2}. \quad (2.6)$$

This function  $h(s, E)$  has a maximum value at  $E_0$  and can be approximated by a delta function:

$$h(s, E) \approx \frac{k_B T}{s} \delta(E - E_0), \quad (2.7)$$

where:

$$E_0 = k_B T \ln\left(\frac{v}{s}\right). \quad (2.8)$$

For the ToF experiment, the photocurrent  $I(t)$  is given by:

$$I(t) = \frac{q\mu_0 F}{L} \int_0^L p(x, t) dx \quad (2.9)$$

which transforms into the Laplace domain as:

$$\hat{I}(s) = I(0) \frac{[1 - \exp(-a(s)t_0)]}{a(s)}, \quad (2.10)$$

with  $I(0) = \frac{q\mu_0 n_0 F}{L}$ .

Differentiating  $\hat{I}(s)$  with respect to  $\ln(s)$ , we obtain:

$$\frac{d}{d \ln(s)} \left( \frac{1}{\hat{I}(s)} \right) = \frac{L}{q n_0 \mu_0 F} \frac{da(s)}{d \ln(s)} B(s), \quad (2.11)$$

where:

$$B(s) = \frac{1 - [1 + a(s)t_0] \exp[-a(s)t_0]}{[1 - \exp(-a(s)t_0)]^2}. \quad (2.12)$$

The localized-state distribution can then be extracted using:

$$g(E_0) = \frac{1}{\sigma_p v_{\text{th}} k_B T} \left[ \frac{1}{B(s)} \frac{d}{d \ln(s)} \left( \frac{I(0)}{\hat{I}(s)} \right) - s \right], \quad (2.13)$$

where  $E_0(s)$  is defined by  $E_0 = k_B T \ln(v/s)$ .

Equation (2.13) provides the theoretical foundation for extracting the DOS in amorphous semiconductors from experimental ToF data. This study applies the Laplace-based formulation to analyze ToF photocurrent data for pure amorphous selenium (a-Se), as reported by Benkhedir et al. [22, 23].

While various techniques exist for estimating the DOS in amorphous semiconductors, the present approach offers a direct, temperature-resolved reconstruction of the conduction band DOS without relying on predefined functional forms or iterative fitting procedures. This provides a complementary perspective to earlier studies and contributes to addressing the scarcity of quantitative DOS data specific to pure a-Se.

## 2.2. Results and discussion

In order to construct a current numerically, we proceeded with the following steps: as well-known, the inverse Laplace of a function is given by:

$$I(t) = \frac{1}{2\pi i} \int_{c-i\infty}^{c+i\infty} I(s)e^{st} dt, \quad (2.14)$$

which  $I(s)$  is defined by equation (2.10).

When we use the following change of variables,  $z = st$ , and  $dz = sdt$ , the integral becomes

$$I(t) = \frac{1}{2\pi i t} \int_{c'-i\infty}^{c'+i\infty} I\left(\frac{z}{t}\right) e^z dz. \quad (2.15)$$

To compute the final integral, we employ the methodology outlined in [6–9]. According to (2.15), the calculated current can be derived as follows: (i) First, we articulate the function  $e^z$  using its Padé approximation expansion; the Padé approximation of a function resembles a Taylor series, but the expansion takes the form of a ratio of two polynomials. (ii) Secondly, we utilize the residue theorem to derive the desired function, namely, the calculated current  $I(t)$ . Consequently, we computed the inverse Laplace transform numerically, employing the Padé approximation, which utilizes rational functions with polynomials of eighth degree. The present work is grounded in the use of the non-monotonous DOS model proposed in [6] as a basis for investigating charge transport properties in stabilized amorphous selenium. The primary objective of this research axis is to evaluate the hole drift mobility by implementing our custom model of localized state distribution. Particular attention is given to amorphous selenium doped with 0.2% and 0.5%, arsenic a composition known to improve thermal stability and widely used in photoconductive materials. To initiate this analysis, the physical quantity utilized in the computation was  $\sigma v_{th} = 10^{-7} \text{ cm}^3 \text{ s}^{-1}$ ,  $v = 10^{12} \text{ s}^{-1}$  and  $k_B = 8.625 \times 10^{-5} \text{ eV K}^{-1}$  is the Boltzmann constant [12]. This simulation serves as a preliminary step toward validating our proposed DOS model.

We are now ready to present and evaluate all the results produced by the Python software used to simulate our currents. Our algorithm was implemented in Python [24]. Figure 1 illustrates the normalized photocurrents over time on a log-log scale for different applied electric fields. For each value of  $F$ , four unique temperatures were examined:  $T = 192, 208, 227$ , and  $238 \text{ K}$ . The illustration distinctly indicates that the transient photocurrent diminishes with time. The transit time is determined at the intersection of the transient photocurrent curve with the time axis [3], which is essential for calculating the mobility as a function of the electric field, a subject that will be discussed in the subsequent section.

Furthermore, as depicted in figure 1, all the curves exhibit analogous behavior in both the pre- and post-transient phases. The image illustrates the ToF transient photocurrents under various applied electric fields, indicating that the transit time is significantly less than the monomolecular recombination lifetime. As the electric field intensifies, the inflection points migrate to shorter time intervals, signifying that these points are associated with the charge-carrier transit time. This facilitates an experimental differentiation: if the inflection point shifts to shorter durations with an increase in the electric field, it can be ascribed to the charge-carrier transit time.

Consequently, drift mobilities can be precisely ascertained, given that the charge-carrier transit time is considerably less than the monomolecular recombination lifetime. This criterion is applicable to non-dispersive transport and is independent of specific physical factors, including  $g(E)$  and  $\mu_0$ .

## 2.3. Determination of localized-state distribution

We aim at demonstrating that the distributions of localized states can be ascertained through the analysis of transient photocurrent. Equation (2.5) is a Fredholm integral equation of the first kind, which may arise from an ill-conditioned problem. The derived density of states (DOS) satisfies all the conditions required to define a generalized solution to such an ill-posed problem and, therefore, necessitates a dedicated resolution method.

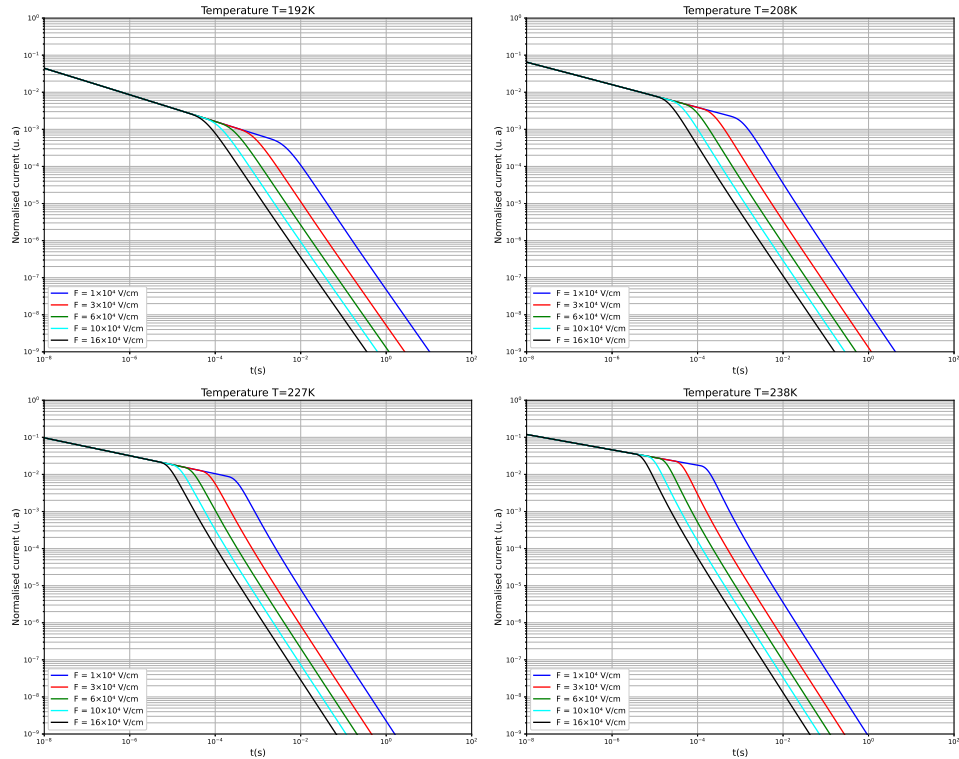


**Figure 1.** (Colour online) Simulated ToF current for the holes in amorphous semiconductors under varying temperatures and electric fields.

In this section, the adopted approach consists in approximating the integration kernel of the equation using a suitably weighted Dirac function. This leads to a simplified expression analogous to equation (2.13).

To assess the effectiveness of the proposed method, we computed the transient current response  $I(t)$  for a representative distribution of traps using our numerical procedure. A Laplace transform was then applied to  $I(t)$  to obtain  $I(s)$ , as defined in equation (2.10), and the DOS was subsequently calculated using equation (2.13).

Figure 2 illustrates the validation process for selecting an appropriate DOS and reconstructing its distribution using our numerical methodology. The localized-state distributions are accurately replicated for  $T_0 > T$ , where the solid lines represent the original DOS at  $T = 300\text{ K}$  used to simulate the transient photocurrents. A strong agreement is observed between the original distributions and those reconstructed using equation (2.13), thereby confirming the reliability and robustness of the proposed Laplace-transform-based method. This result validates our ability to extract the DOS in pure a-Se and provides a solid foundation for investigating deeper charge transport mechanisms in amorphous semiconductors.

Building on this framework, we conducted an extensive investigation using the ToF technique — widely recognized for its capability to probe the dynamics of charge carriers in disordered materials. ToF measurements were performed over a wide range of temperatures (from  $-40^\circ\text{C}$  to  $+23^\circ\text{C}$ ) to analyze the distribution of trap states within the conduction band tail of pure amorphous selenium.

Figure 3 presents the reconstructed localized-state distributions derived from ToF transient photocurrent data. These profiles deviate from a simple exponential decay and instead exhibit a Gaussian-like shape. Two distinct features are observed:

- A shallow trap peak appearing in the range  $E - E_c \approx 0.28 - 0.30\text{ eV}$ , which is clearly visible at low temperatures ( $-40^\circ\text{C}$ ,  $-25^\circ\text{C}$ ). At these temperatures, reduced thermal energy limits the carrier access to states near the conduction band edge, enhancing the visibility of shallow traps.

- A deeper trap peak centered around  $E - E_c \approx 0.45 - 0.50$  eV, which becomes increasingly prominent at higher temperatures (from  $-10^\circ\text{C}$  to  $+23^\circ\text{C}$ ), as carriers gain sufficient thermal energy to populate and escape the deeper localized states.

Furthermore, the position of the shallow trap level, identified in the present study near 0.30 eV below the conduction band mobility edge, is in excellent agreement with the values derived from pre-transit photocurrent analyses. Specifically, earlier studies have reported a shallow defect state energy of  $E_{\text{se}} = 0.28 \pm 0.02$  eV, extracted from the early-time regime of ToF measurements [18]. This state reflects a population of shallow traps that govern the carrier behaviour before transit. The excellent agreement with our reconstructed DOS confirms the accuracy of the Laplace-transform method in resolving the energy distributions near the conduction edge.

These temperature-dependent variations provide crucial insight into the thermal activation dynamics of carriers and confirm the presence of energetically distinct trapping centers. The position and nature of these two peaks are in excellent agreement with earlier findings, which revealed similar defect states near 0.30 eV and 0.45 – 0.50 eV in a-Se through numerical simulations of ToF photocurrents [20]. However, unlike their study, our broader temperature range and time resolution allow for a more accurate resolution of these defect states, and do not indicate the presence of additional deep states below 0.6 eV. The discrepancy probably arises from the experimental limitations in their work — namely, a narrow time window centered around the transit time and measurements performed exclusively at room temperature — conditions that are insufficient to isolate contributions from deeper levels.

Importantly, the results of the present study reveal a remarkable symmetry in the distribution of localized states between the valence and conduction band tails in amorphous selenium. The reconstructed DOS, extracted via Laplace-transform analysis from ToF data, displays comparable energetic spreads and defect densities on both sides of the mobility gap. This symmetry strongly suggests that analogous trapping and release mechanisms govern the transport of both electrons and holes, reflecting the intrinsic structural disorder of the amorphous matrix.

This observation directly complements our earlier work [6], in which we focused on the valence band side of pure a-Se. In that study, we applied the same Laplace-transform technique to transient photoconductivity (TPC) measurements and revealed a non-monotonous DOS profile with two discrete defect levels:

- A shallow level approximately 0.30 eV above the valence band edge ( $E_v$ ), associated with local structural distortions such as dihedral angle variations.
- A deeper level near 0.45 eV, attributed to the presence of  $D^-$  centers, in agreement with the negative- $U$  model [15, 18].

As in the conduction side study, the shallow level in the valence band is more prominent at low temperatures, while the deeper level becomes significant at elevated temperatures — demonstrating a consistent temperature dependence of trap activation across both band edges.

Furthermore, we extended this investigation to arsenic-doped a-Se. In this context, shallow defects disappeared and deeper levels became dominant. This behavior was attributed to arsenic atoms having modified the local bonding environment, which led to a smoother distribution of localized states in the valence band tail. Using a least-squares fitting procedure, we reconstructed the DOS profiles for samples doped with 0.2% and 0.5% As, achieving high accuracy in replicating experimental photocurrents.

Taken together, these studies — both performed by the present authors — provide a comprehensive insight into the energetic structure of the localized states in a-Se. The symmetric and structured distribution of states on both sides of the mobility gap demonstrates that trapping phenomena are energetically balanced for electrons and holes. This balance has significant implications for the modelling of carrier transport in amorphous semiconductors and supports the use of unified descriptions of localized states across both the conduction and valence bands.

An essential aspect of analyzing the transport characteristics in amorphous selenium is the precise assessment of carrier drift mobility and lifetime  $\tau$ . Multiple studies have emphasized the scientific and technological significance of these factors [11, 12]. To deepen this understanding and support our experimental findings, we implemented numerical simulations of hole transport in stabilized amorphous selenium. The simulations aimed at reproducing and interpreting photocurrent transients, allowing for a detailed investigation of the temperature and field dependence of hole mobility.

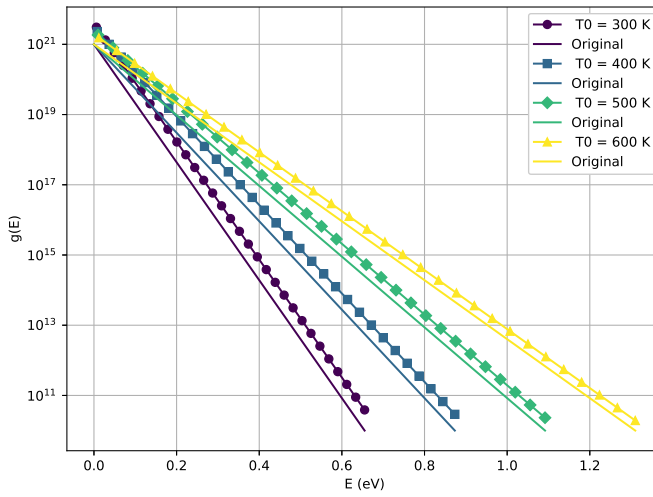


**Figure 2.** (Colour online) Localized-state distributions determined from the numerically calculated ToF transient photocurrent. The solid lines are original distributions at  $T = 300$  K for numerical calculation of the transient photocurrent using equation (2.13).

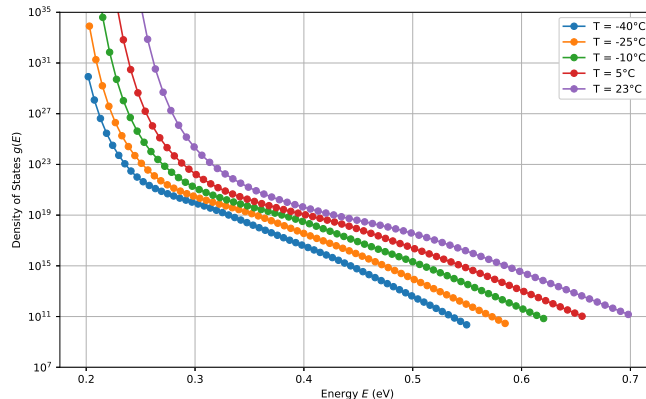


**Figure 3.** (Colour online) Localized-state distributions of the pure a-Se determined from the numerically calculated ToF transient photocurrent [22, 23]

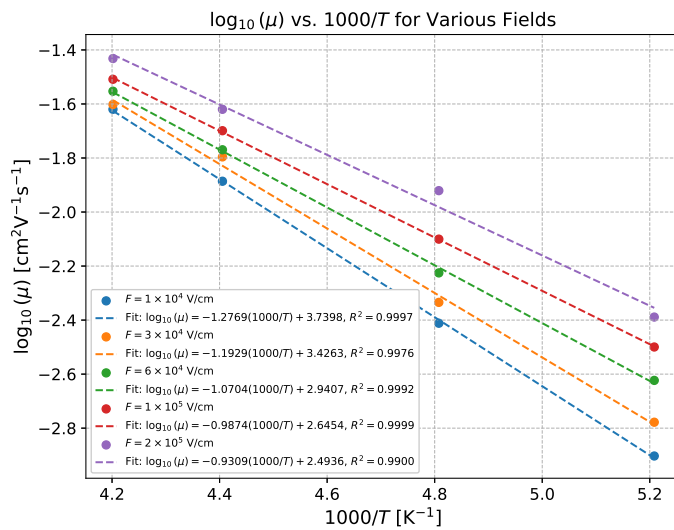
### 3. Simulation of hole mobility in amorphous semi-conductors

We additionally corroborated the non-monotonous model of the localized state density distribution using the simulation of hole photocurrents. In this instance, we sought to resolve the continuity equations under various scenarios. The first objective was to replicate transient ToF photocurrents utilizing the identical functions for the localized state density distribution as specified in the preceding equations.

Our inverse Laplace software enabled us to acquire currents for various temperatures and fields. The aim is to assess the hole mobility in stabilized a-Se. This section employs a widely recognized method from the literature, which involves calculating the transit time from the simulated ToF currents at a specified temperature and field utilized in prior experimental investigations. The hole mobility  $\mu_h$  can be

**Table 1.** Simulated hole mobility in stabilized a-Se.

F(V/cm)	$10^4$	$3 \times 10^4$	$6 \times 10^4$	$10^5$	$1.6 \times 10^5$
$\mu_h(T = 192\text{K}) (\text{cm}^2\text{V}^{-1}\text{s}^{-1})$	0.00125	0.001667	0.002381	0.003165	0.004085
$\mu_h(T = 208\text{K}) (\text{cm}^2\text{V}^{-1}\text{s}^{-1})$	0.003876	0.00463	0.005952	0.007937	0.012
$\mu_h(T = 227\text{K}) (\text{cm}^2\text{V}^{-1}\text{s}^{-1})$	0.013	0.016	0.017	0.02	0.024
$\mu_h(T = 238\text{K}) (\text{cm}^2\text{V}^{-1}\text{s}^{-1})$	0.024	0.025	0.028	0.031	0.037

**Figure 4.** (Colour online) Logarithm of hole mobility as a function of inverse temperature for various electric fields.

derived using the subsequent equation [25–27]:

$$\mu_h = \frac{L}{t_r F}, \quad (3.1)$$

where  $L$  denotes the sample thickness and  $t_r$  signifies the transit time. The transit time was determined using the tangent intersection method, by identifying the point where linear fits to the pre-transit and post-transit regions of the ToF current curve intersect.

All computations in this study were executed in this manner. The simulated mobility values for the two samples under varying field and temperature conditions are presented in table 1. The correlation between mobility and  $T^{-1}$  is accurately represented by a linear regression.

We utilize Arrhenius plots to ascertain the activation energy. The Arrhenius plots of mobility clearly demonstrate that temperature substantially influences the values of  $\mu$ . The Arrhenius plot is a prevalent analytical instrument in semiconductor physics, utilized to investigate the temperature dependence of charge carrier mobility. This graphic depicts the logarithm of mobility ( $\log \mu$ ) against the inverse of temperature ( $1/T$ ). It is extensively utilized to calculate activation energies and comprehend the temperature-dependent characteristics of charge transport.

The correlation between mobility ( $\mu$ ) and temperature ( $T$ ) often adheres to an exponential model.

$$\mu = \mu_0 \exp\left(-\frac{E_a}{k_B T}\right), \quad (3.2)$$

where:  $\mu_0$  denotes the pre-exponential factor (mobility at infinite temperature) and  $E_a$  represents the activation energy.

**Table 2.** Activation energy values.

V( volt )	50	150	300	500	800
$F$ ( V/cm)	$10^4$	$3 \times 10^4$	$6 \times 10^4$	$10 \times 10^4$	$16 \times 10^4$
$E_h$ (eV)	0.254	0.237	0.213	0.196	0.185

Applying the logarithm to both sides results in:

$$\log \mu = \log \mu_0 - \frac{E_a}{k_B T}. \quad (3.3)$$

The slope of the Arrhenius plot ( $\log \mu$  vs  $1/T$ ) in this linearized format can be utilized to ascertain the activation energy  $E_a$ . The activation energy denotes the thermal energy required for charge carriers to surmount obstacles like traps or flaws inside the material. The Arrhenius figure elucidates the relationship between mobility and temperature variations. In numerous amorphous semiconductors, such as a-Se (amorphous selenium), mobility generally rises with temperature, signifying a thermally triggered transport mechanism. Essential points to consider:

- i) A steeper slope on the Arrhenius plot indicates a greater activation energy, signifying more pronounced trapping or scattering effects.
- ii) A smaller slope suggests reduced activation energy, potentially signifying fewer traps or more extensive states that facilitate improved carrier delocalization.

In amorphous semiconductors such as a-Se, the Arrhenius plot is commonly utilized to investigate the hole mobility. It can furnish critical insights regarding localized states, the DOS, and the effects of doping (e.g., arsenic doping). Fluctuations in the slope or departures from a linear trajectory may signify shifts between distinct charge transport regimes, such as from non-dispersive to dispersive transport. The Arrhenius plot of mobility is an effective instrument for examining the charge transport pathways in disordered materials. It facilitates the extraction of essential data, such as activation energy, and clarifies the influence of temperature on mobility, providing enhanced understanding of the electrical structure of amorphous semiconductors.

Return to our case now. To investigate the temperature dependence of hole mobility, we plot  $\log \mu$  as a function of the inverse temperature ( $1/T$ ) for each applied electric field, as shown in figure 4. This representation reveals a temperature-dependent variation in mobility and provides a clearer interpretation of the thermally activated transport mechanism.

The temperature dependence of hole mobility as a function of the inverse temperature  $1/T$  is well approximated by a linear relationship. Arrhenius plots clearly demonstrate that temperature has a significant influence on mobility. Within the temperature range of 192 K to 238 K, mobility increases with temperature, in excellent agreement with previously reported results [28]. From the linear regressions of the  $\log \mu$  versus  $1/T$  curves, activation energies were extracted from the slopes of the linear regions. Additionally, variations in these slopes under different electric field strengths highlight the field dependence of the activation energy. The extracted values are summarized in table 2. The high correlation coefficients confirm that the hole mobility in both studied samples exhibits an exponential dependence on temperature. Moreover, the analysis of the mobility variation with respect to electric field at different temperatures reveals that the activation energies are field-dependent. This behaviour is indicative of the Poole-Frenkel effect, which describes the field-assisted thermal emission of charge carriers from localized trap states.

The Poole-Frenkel coefficient  $\beta_{PF}$  is a parameter that characterizes the field-induced reduction of the potential barrier for charge carriers confined in localized states within insulating or semiconducting materials [29]. It provides an insight into the defect structure of the material and the mechanisms governing the charge transport by quantifying how an electric field facilitates the release of the trapped carriers. The effect occurs when an applied electric field lowers the energy barrier associated with a Coulombic trap — a localized defect that attracts a charge — thereby increasing the probability of carrier escape and enhancing electrical conduction.

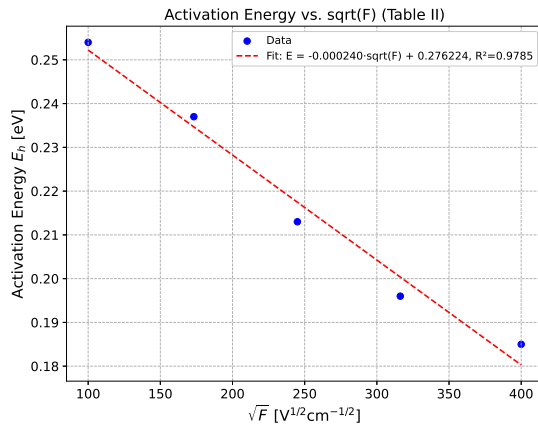


**Figure 5.** (Colour online) Variation of activation energy as a function of the electric field.

The Poole-Frenkel effect is typically expressed by the subsequent relationship:

$$\mu = \mu_0 \exp \left( -\frac{E_a - \beta_{PF} \sqrt{F}}{k_B T} \right), \quad (3.4)$$

where:  $\mu$  represents mobility,  $\mu_0$  denotes the pre-exponential factor,  $E_a$  signifies the activation energy at zero field, and  $\beta_{PF}$  indicates the Poole-Frenkel coefficient. The Poole-Frenkel coefficient is expressed as follows:

$$\beta_{PF} = \sqrt{\frac{q^3}{\pi \epsilon_0 \epsilon_r}}, \quad (3.5)$$

where  $q$  denotes the elementary charge ( $1.6 \times 10^{-19}$  C),  $\epsilon_0$  represents the vacuum permittivity ( $8.854 \times 10^{-12}$  F/m), and  $\epsilon_r$  signifies the relative permittivity of the material.

In our results, the activation energy decreases from 0.254 eV to 0.185 eV. When these values are fitted to the Poole-Frenkel relation, a linear dependence on  $F^{1/2}$  is observed, as shown in figure 5. The slope of the linear fit yields a Poole-Frenkel coefficient of  $\beta_{PF} = 2.4 \times 10^{-4}$  eV (V cm<sup>-1</sup>)<sup>-1/2</sup>, and the extrapolated activation energy at zero field is approximately 0.28 eV. These results provide strong evidence that charge transport in the studied material is dominated by a field-assisted thermal emission mechanism.

It is physically significant to note that similar field-dependent behaviors of activation energy have been reported in prior studies. In the case of undoped amorphous selenium, an activation energy of  $0.28 \pm 0.02$  eV was observed at temperatures below 250 K [26], indicating a thermally activated transport regime. For stabilized (arsenic-doped) amorphous selenium, the reported activation energy was approximately 0.21 eV [28], which is in close agreement with the value extracted in the present work. Moreover, the Poole-Frenkel coefficient  $\beta_{PF}$  reported in [19] estimated as  $\beta_{PF} = 2.7 \times 10^{-4}$  eV (V/cm)<sup>-1/2</sup> is in good agreement with the value deduced in this study and corresponds to the doped case. This consistency reinforces the interpretation that hole transport occurs via field-assisted thermal emission from localized trap states. The same study [19] also supports the presence of a non-monotonous density of localized states near the valence band edge, further validating our theoretical approach.

## 4. Conclusion

In this study, we performed a comprehensive numerical investigation of charge transport in amorphous selenium (a-Se) based on a Laplace-transform analysis of ToF transient photocurrents. The reconstructed DOS on the conduction band side in pure a-Se revealed a symmetric distribution with respect to the

valence band side, as established in our previous studies, indicating balanced trapping dynamics across the mobility gap.

To validate the transport mechanisms, we simulated the hole mobility using a known DOS model for stabilized a-Se. The simulated data exhibited an Arrhenius-type temperature dependence, with activation energies decreasing from approximately 0.25 eV at low fields to 0.18 eV at higher fields. The extracted Poole-Frenkel coefficient,  $\beta_{\text{PF}} = 2.4 \times 10^{-4} \text{ eV (V/cm)}^{-1/2}$ , supports the interpretation that the hole transport is governed by field-assisted thermal emission from localized states.

The agreement between our simulation results and established experimental data confirms the robustness of the proposed model and method.

## References

1. Spear W. E., Proc. Phys. Soc., 1960, **76**, 826, doi:10.1088/0370-1328/76/6/302.
2. Schmidlin F. W., Phys. Rev. B, 1977, **16**, 2362, doi:10.1103/PhysRevB.16.2362.
3. Noolandi J., Phys. Rev. B, 1977, **16**, 4466, doi:10.1103/PhysRevB.16.4466.
4. Schmidlin F. W., Philos. Mag. B, 1980, **41**, 535, doi:10.1080/13642818008245405.
5. Kastner M. A., Solid State Commun., 1983, **45**, 191, doi:10.1016/0038-1098(83)90374-5.
6. Serdouk F., Benkhedir M. L., Physica B, 2015, **459**, 122, doi:10.1016/j.physb.2014.12.002.
7. Serdouk F., Boumali A., Makhlof A., Benkhedir M. L., Rev. Mex. Fis., 2020, **66**, 643–655, doi:10.31349/RevMexFis.66.643.
8. Serdouk F., Boumali A., Sibatov R. T., Fractal Fract., 2023, **7**, 243, doi:10.3390/fractfract7030243.
9. Goutal Y., Serdouk F., Boumali A., Benkhedir M. L., Theor. Math. Phys., 2024, **219**, 839–855, doi:10.1134/S0040577924050118.
10. Ohno A., Hanna J., Dunlap D. H., Jpn. J. Appl. Phys., 2008, **47**, 1079, doi:10.1143/JJAP.47.1079.
11. Naito H., Ding J., Okuda M., Appl. Phys. Lett., 1994, **64**, 1830, doi:10.1063/1.111769.
12. Naito H., Nagase T., Ishii T., Okuda M., Kawaguchi T., Maruno S., J. Non-Cryst. Solids, 1996, **363**, 198–200, doi:10.1016/0022-3093(95)00725-3.
13. Ogawa N., Nagase T., Naito H., J. Non-Cryst. Solids, 2000, **367**, 266–269, doi:10.1016/S0022-3093(99)00732-2.
14. Nagase T., Naito H., J. Non-Cryst. Solids, 1998, **824**, 227–230, doi:10.1016/S0022-3093(98)00163-X.
15. Benkhedir M. L., Aida M. S., Adriaenssens G. J., J. Non-Cryst. Solids, 2004, **344**, 193, doi:10.1016/j.jnoncrysol.2004.08.062.
16. Benkhedir M. L., Brinza M., Adriaenssens G. J., J. Phys.: Condens. Matter, 2004, **16**, No. 44, S5253, doi:10.1088/0953-8984/16/44/022.
17. Qamhieh N., Benkhedir M. L., Brinza M., Willekens J., Adriaenssens G. J., J. Phys.: Condens. Matter, 2004, **16**, No. 23, 3827, doi:10.1088/0953-8984/16/23/003.
18. Benkhedir M. L., Brinza M., Adriaenssens G. J., Main C., J. Phys.: Condens. Matter, 2008, **20**, 215202, doi:10.1088/0953-8984/20/21/215202.
19. Benkhedir M. L., Djefaflia F., Mansour M., Qamhieh N., Phys. Status Solidi C, 2010, **7**, No. 3–4, 877–880, doi:10.1002/pssc.200982846.
20. Koughia K., Shakoor Z., Kasap S. O., Marshall J. M., J. Appl. Phys., 2005, **97**, No. 3, 033706, doi:10.1063/1.1835560.
21. Kasap S., Koughia C., Berashevich J., Johanson R., Reznik A., J. Mater. Sci.: Mater. Electron., 2015, **26**, 4644–4658, doi:10.1007/s10854-015-3069-1.
22. Benkhedir M. L., Defect Levels in the Amorphous Selenium Band Gap, Ph.d. thesis, Katholieke Universiteit Leuven, Belgium, 2006.
23. Emelianova E. V., Benkhedir M. L., Brinza M., Adriaenssens G. J., J. Appl. Phys., 2006, **99**, No. 8, 083702, doi:10.1063/1.2187395.
24. van Rossum G., Drake F. L., Python 3 Reference Manual, CreateSpace, Scotts Valley, CA, 2009.
25. Gill W. D., J. Appl. Phys., 1972, **43**, 5033, doi:10.1063/1.1661065.
26. Marshall J. M., Owen A. E., Phys. Status Solidi A, 1972, **12**, 181, doi:10.1002/pssa.2210120119.
27. Kasap S. O., Juhasz C., J. Phys. D: Appl. Phys., 1985, **18**, 703, doi:10.1088/0022-3727/18/4/015.
28. Fogal B., Kasap S., Can. J. Phys., 2014, **92**, No. 7, 634–639, doi:10.1139/cjp-2013-0524.
29. Hill R. M., Philos. Mag., 1971, **23**, 59, doi:10.1080/14786437108216365.

## **Дослідження густини станів та рухливості носіїв заряду в аморфних напівпровідниках за допомогою аналізу фотоструму за часом прольоту (ToF)**

Ф. Сердук, А. Бумалі, М. Л. Бенхедір, І. Гутал

Лабораторія теоретичної та прикладної фізики, Університет Ешахіда Шейха Ларбі Тебессі, Тебесса, Алжир

У даному дослідженні розглядаються характеристики електронного переносу аморфних напівпровідників за допомогою вимірювань часу прольоту (ToF) та числового моделювання. Основною метою є визначення густини станів (DOS) в аморфному селені (a-Se) та оцінка залежності рухливості дірок від температури та електричного поля. Комплексне дослідження локалізованих станів у межах щілини рухливості проведено за допомогою перетворення Лапласа для переходних процесів фотоструму ToF у поєднанні з моделлю множинних пасток. Такий підхід дозволяє точно реконструювати DOS у широкому діапазоні температур, що уможливлює чітку ідентифікацію поверхневих та внутрішніх пасток та виявлення термічно активованих механізмів переносу. Модельовані струми ToF також використовуються для оцінки рухливості дрейфу дірок за різних температурних та польових умов. Енергії активації отримані з графіків Арреніуса для значень рухливості. Результати підтверджують фізично узгоджений опис електронної структури в a-Se а також застосовність методів на основі перетворення Лапласа для вивчення переносу заряду в невпорядкованих напівпровідниках.

**Ключові слова:** аморфний селен (a-Se), час прольоту (ToF), переходний фотострум (TPC), перетворення Лапласа, модель множинного захоплення (MTM), густина станів (DOS)

---

---